Simulation and active control of chatter in milling via a mechatronic simulator

A. Ganguli*, A. Deraemaeker, I. Romanescu, M. Horodinca, A. Preumont
Active Structures Lab, Université Libre de Bruxelles, CP 165/42, Brussels, Belgium.
*Corresponding Author e-mail: abhijit.ganguli@gmail.com

Abstract

This paper presents a 2 DOF "Hardware in the Loop" mechatronic simulator for the study of regenerative chatter in milling. The main motivation behind the construction of the simulator is to propose active damping as a strategy to stabilize chatter in milling. A good comprehension of regenerative chatter in milling is essential for that purpose. Characterization of chatter in a real machining environment may be difficult. The mechatronic simulator provides an alternative way to conduct investigations on chatter in milling in a laboratory environment, without conducting actual cutting tests. The simulator is found to simulate realistically various kinds of bifurcation phenomena, normally expected in milling operations. Active damping is then implemented on the system to investigate its effect on stability. It is shown experimentally that stability lobes are enhanced due to application of active damping, which fulfils the original objective of proposing active damping as a chatter stabilizing strategy.

Keywords: Milling, Chatter simulator, Active Damping

1 Introduction

The chatter phenomenon is a vibrational instability in the metal cutting process, which affects the efficiency of the cutting process by reducing the metal removal rate (MRR) and the life of the cutting tool. Chatter has been a popular topic of industrial research for quite some time. The regenerative theory of chatter, proposed independently by Tobias and Fishwick (1958a) and Tlusty and Polacek (1963), forms the theoretical foundation of

research on chatter. The regenerative process is described in Figure 1 for a single degree of freedom (SDOF) turning operation, involving a rotating cylindrical workpiece and a cutting tool. If the system is rigid, the thickness of chip removed from the surface is h_0 which is called the feed of the tool into the workpiece. While machining, the flexible tool may face a hard spot on the surface of the workpiece and some vibrations are triggered. This leaves behind a wavy surface, as shown in the figure and after one full rotation the tool faces the waves left during the previous pass. Therefore, according to Figure 1, the dynamic chip thickness is given by,

$$h(t) = h_0 + y(t - T) - y(t) \tag{1}$$

where y and $y(t - T)$ are displacements during the current and previous pass of the tool, $T = 60/N$ is the time of one revolution of the workpiece and N is the spindle speed in RPM. Assuming that the cutting forces are proportional to the frontal area of the chip, the cutting force in the Y direction is equal to

$$F_c(t) = K_f.a.[h_0 + y(t - T) - y(t)] \tag{2}$$

where K_f is the cutting force constant, a is the axial width of cut, measured perpendicular to the plane of Figure 1. The tool now encounters a dynamic excitation force, which generates more vibration waves on the workpiece surface. These waves continue to modulate the chip thickness one revolution later. If the vibrations keep on increasing, an unstable situation accompanied by loud noise is encountered. Merrit (1965) models this process in the form of a feedback loop interaction between the cutting mechanics and the structural dynamics of the machine tool system as shown in Figure 2. The study provides a control engineering viewpoint of chatter instability. Defining $G(s)$ as the system transfer function between the force F_c and the displacement y, Laplace transforming Equ. 2 and neglecting the term due to the feed due to the fact that this is a linear analysis, we get the following equation.

$$F_c(s) = K_f a(e^{-sT} - 1)G(s)F_c(s) \tag{3}$$

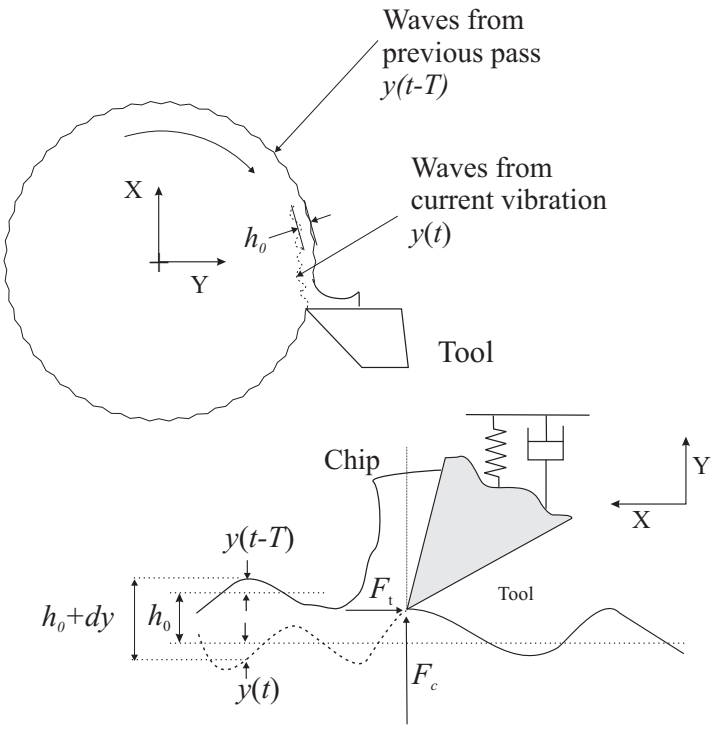

Figure 1: The regeneration process

Here $y(t-T)$ is substituted as $y(s)e^{-sT}$ in Laplace domain. From Equ. 3, the characteristic equation for turning can be written as,

$$1 + K_f a(1 - e^{-sT})G(s) = 0 \tag{4}$$

At the limit of stability, for a particular combination of the axial depth of cut a and spindle rotation period T, at least a pair of conjugate roots of the characteristic equation may lie on the imaginary axis. This value of a corresponds to the limit of stable machining for the chosen spindle speed. A plot of the maximum axial width of cut for stable machining for different spindle speeds is called the stability lobe diagram. A typical stability lobe diagram is shown in Figure 3. The area below the curve denotes chatter free machining and the region above denotes the unstable region. The straight line joining the minimum value of the stability limit on the different lobes is called the Asymptotic Level of stability and this level varies approximately as $2\xi(1+\xi)$, where ξ is the structural damping ratio.

Chatter in milling is more complicated than turning, due to the involvement of multiple teeth in the cutting process and the changing directions of the cutting forces as the

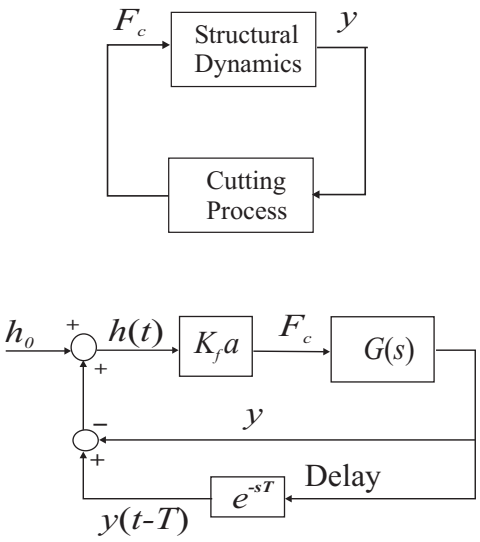

Figure 2: Merrit's model for chatter in turning

cutter rotates inside the cut. Chatter in turning is governed by a delay differential equation (DDE) with constant coefficients, whereas in milling, the system is governed by a DDE with periodic coefficients. Frequency domain techniques cannot be applied as in the case of the time invariant turning example. This has forced many researchers to study the stability aspects of milling in time domain. Tlusty and Ismail (1983) generate stability lobe diagrams for milling, based on time domain simulations. The main objective behind this work is to propose active damping as a strategy for chatter stabilization in milling. A good understanding of the phenomenon and its various aspects are essential for that purpose. Experimental investigations on chatter via real metal cutting tests may be difficult, due to the involvement of numerous parameters in the cutting process. In this paper a simplified approach is proposed to demonstrate the phenomenon experimentally. The authors present a mechatronic simulator, developed using the "Hardware in the Loop" concept for chatter simulation in milling, which is able to reproduce the various aspects of the instability realistically. Active damping is then implemented as a control strategy on the simulator to check whether stabilization of chatter is possible. The paper is organized as follows. Section 2 deals with the mathematical formulations of dynamic regenerative model of chatter in milling, which are used in the simulator. Section 3 presents various methods of stability analysis in literature to develop a background on chatter in milling and to demonstrate the different mechanisms of chatter, as reported by other authors. Section 4 discusses about the experimental setup and numerical and experimental inves-

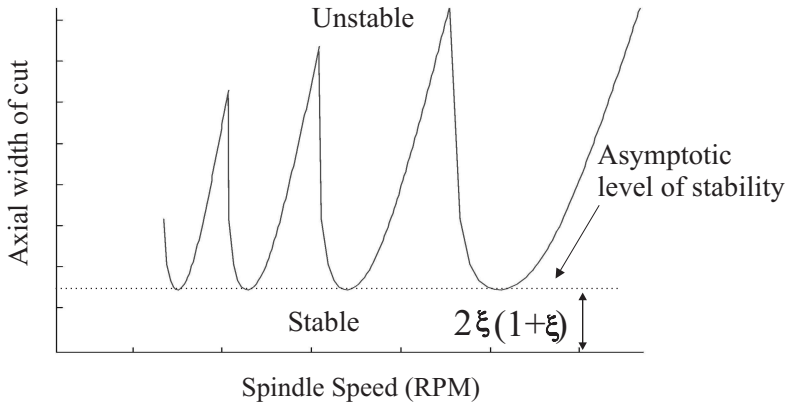

Figure 3: A typical stability lobe diagram

tigations on the system. Stability lobe diagrams are presented by numerical time domain simulations, using an identified model of the structure and the mathematical model of regenerative chatter, developed in Section 2. The results are compared to show the capability of the setup to simulate real chatter situations. The effect of active damping on the stabilization of chatter instability is investigated in Section 5.

2 The dynamic milling system

Three kinds of milling operations are shown in Figure 4: upmilling, downmilling and slotting. The intercept of the arc through which a cutting tool rotates inside the cut on the vertical axis is called the radial depth of cut. If the radial depth is equal to the diameter of the tool, as in the case of slotting, the radial immersion is 100%. 50% immersion means that the radial depth of cut is half of the diameter of the cutting tool and the angle of cut is therefore 90 degrees. Radial immersions for which the angle of the cut is very low are called low immersion milling operations. Figure 5 a) shows a 2D flexible milling tool. The tool is assumed to be non helical. In case of a rigid cutter and workpiece system, the metal removed by a tooth can be approximated by the area between the dotted lines, as shown in Figure 5 a). However, due to general flexibility of the tool workpiece system, vibration of the tool occurs. Each tooth leaves a wavy surface, which is encountered by the subsequent tooth. This causes the fluctuation of the cutting force and further excites the structure. With each pass of the tooth, if the vibrations increase, the chatter instability is triggered. This is the regeneration process in the milling operation.

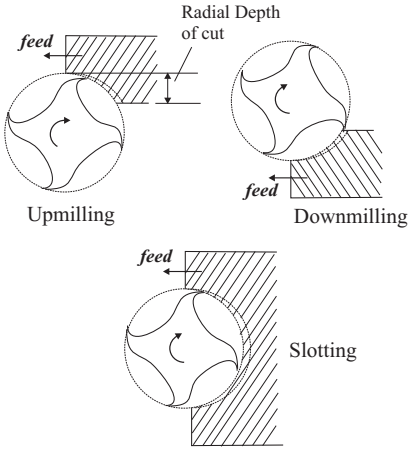

Figure 4: Different kinds of milling operations

As shown in Figure 5 b), let f_t, be the horizontal motion of the tool into the workpiece, also called the feed. Assuming that the diameter of the tool is much larger compared to the feed, the thickness of the metal encountered by a single tooth can be assumed to be the small strip between the two circular arcs. Then the chip thickness in the radial direction is approximated by,

$$h_0 = f_t \sin\theta \tag{5}$$

Referring to Figure 5 a), the i-th tooth is acted upon by an orthogonal system of forces, F_{ti}, which is the tangential component and F_{ri}, which acts in the radial direction. Following Altintas (2000), the force encountered by the milling tooth is taken proportional to the instantaneous chip thickness.

$$\left\{ \begin{array}{c} F_{ti} \\ F_{ri} \end{array} \right\} = \left[\begin{array}{c} K_t.h_0.a \\ K_r.F_{ti} \end{array} \right] \tag{6}$$

where K_t and K_r are the tangential and the radial cutting constants and a is the axial width of cut, measured perpendicular to the plane of Figure 5.

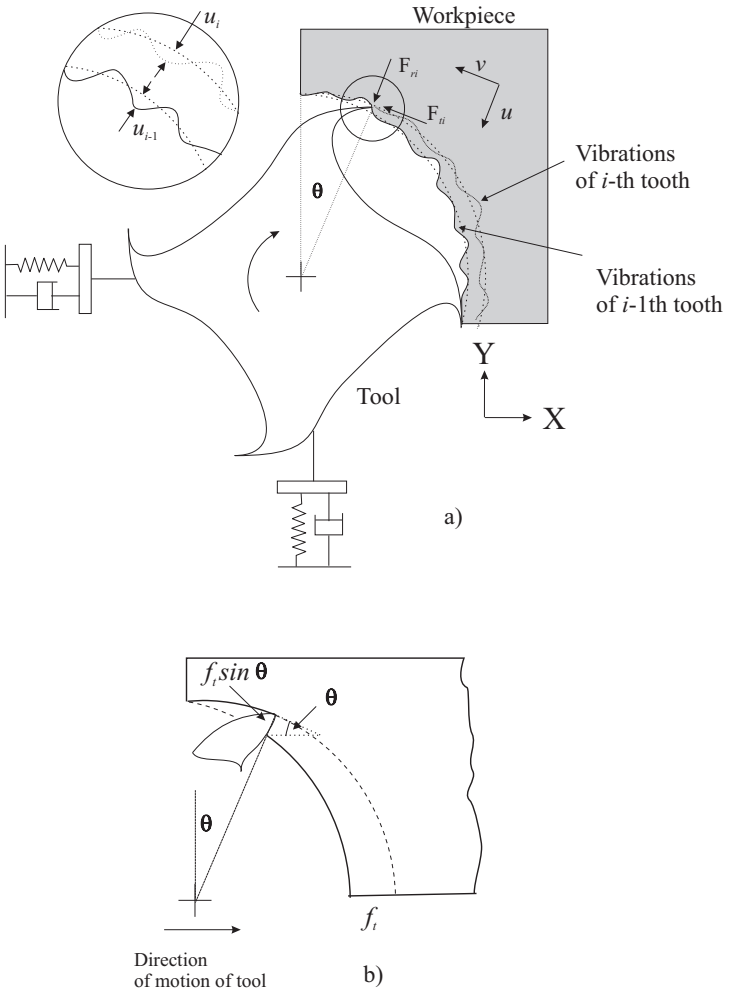

Figure 5: a) A flexible 2 DOF milling tool system b) Horizontal feed in milling

From figure 5 a), it is observed that the direction of the instantaneous tangential and radial forces on a cutting tooth depend on the location of the tooth in the cut. The total force acting on the milling tool in the direction of flexibilities, i.e., the **X** and **Y** directions, is the sum of the contributions of the total number of teeth inside the cut. Early models of milling did not consider the changing direction of the cutting forces and considered an average direction of the forces. Sridhar et al. (1968a) and (1968b) incorporate the varying direction of the cutting forces in their detailed formulation of the milling forces. Considering Figure 5 a), **X** and **Y** are the global axes of reference and θ is the instantaneous position of the i- th tooth of the cutter. Let the displacements in the radial and the tangential directions be u_i and v_i respectively. Considering the regeneration

effect, which is shown magnified in the circle in Figure 5 a), the instantaneous uncut radial chip thickness is,

$$h(\theta) = f_t \sin\theta + u_{i-1} - u_i \tag{7}$$

where u_i and u_{i-1} are the deflections of the i- th tooth and the $i-1$ th tooth respectively. Here $u_{i-1} = u(t-T)$ where T is the tooth passing period, as given by Equ. 8.

$$T = \frac{60}{nN} \tag{8}$$

where N is the spindle speed and n is the total number of teeth. Expressing the displacement u in terms of the global displacements x and y of the cutter,

$$u_i = -x\sin\theta - y\cos\theta$$

$$u_{i-1} = -x(t-T)\sin\theta - y(t-T)\cos\theta \tag{9}$$

Using Equ. 9, the radial chip thickness can be expressed as,

$$h(\theta) = f_t \sin\theta + \begin{bmatrix} \sin\theta & \cos\theta \end{bmatrix} \begin{Bmatrix} x(t) - x(t-T) \\ y(t) - y(t-T) \end{Bmatrix} \tag{10}$$

Therefore, referring to Equ. 6, the tangential and radial cutting forces acting on the i-th tooth are expressed as,

$$\begin{Bmatrix} F_{t_i} \\ F_{r_i} \end{Bmatrix} = \begin{bmatrix} K_t.h(\theta).a \\ K_r.K_t.h(\theta).a \end{bmatrix} \tag{11}$$

Transforming to global coordinates, the forces are,

$$\begin{Bmatrix} F_{x_i} \\ F_{y_i} \end{Bmatrix} = \begin{bmatrix} -\cos\theta & -\sin\theta \\ \sin\theta & -\cos\theta \end{bmatrix} \begin{Bmatrix} F_{t_i} \\ F_{r_i} \end{Bmatrix} \tag{12}$$

Substituting equations 10 and 11 in Equ. 12, the system of forces, acting on the i-th tooth, in the **X** and **Y** directions are,

$$\begin{Bmatrix} F_{x_i} \\ F_{y_i} \end{Bmatrix} = \begin{Bmatrix} -K_t\cos\theta\sin\theta - K_tKr\sin^2\theta \\ -K_t\sin^2\theta - K_tKr\sin\theta\cos\theta \end{Bmatrix} f_t.a$$

$$+\begin{bmatrix} -K_t\sin\theta\cos\theta - K_tK_r\sin^2\theta & -K_t\cos^2\theta - K_tK_r\sin\theta\cos\theta \\ K_t\sin^2\theta - KtK_r\sin\theta\cos\theta & K_t\sin\theta\cos\theta - K_tK_r\cos^2\theta \end{bmatrix}\begin{Bmatrix} x(t)-x(t-T) \\ y(t)-y(t-T) \end{Bmatrix} \tag{13}$$

Since milling involves multiple teeth in the cut, the total force in the two directions is the summation of the contributions from each tooth. This is shown in Equ. 14. Substituting $x(t) - x(t-T) = \Delta x$ and $y(t) - y(t-T) = \Delta y$ and summing up the contributions of n teeth, the forces in the x and y directions are,

$$\begin{Bmatrix} F_x \\ F_y \end{Bmatrix} = K_t.a.\sum_{i=1}^{n}\left(\begin{Bmatrix} \alpha_{11i} \\ \alpha_{21i} \end{Bmatrix}.f_t + \begin{bmatrix} \alpha_{11i} & \alpha_{12i} \\ \alpha_{21i} & \alpha_{22i} \end{bmatrix}\begin{Bmatrix} \Delta x \\ \Delta y \end{Bmatrix}\right)g(\theta_i) \tag{14}$$

where

$$\alpha_{11i} = \frac{1}{2}[-\sin 2\theta_i - K_r(1-\cos 2\theta_i)]$$

$$\alpha_{11i} = \frac{1}{2}[-(1+\cos 2\theta_i) - K_r\sin 2\theta_i]$$

$$\alpha_{21i} = \frac{1}{2}[(1-\cos 2\theta_i) - K_r\sin 2\theta_i]$$

$$\alpha_{22i} = \frac{1}{2}[\sin 2\theta_i - K_r(1+\cos 2\theta_i)]$$

$$\theta_i = \theta + (i-1)2\pi/n \tag{15}$$

The function $g(\theta_i)$ denotes whether a tooth is inside the cut or not. $g(\theta_i) = 1$ for $\theta_{entry} < \theta_i < \theta_{exit}$ and zero elsewhere, where θ_{entry} and θ_{exit} are the angles of entry and exit respectively. Therefore, expressing the displacement vector as $\mathbf{x} = [x\,y]^T$ and $K_{cut} = K_t.a$, the general form of the forces can be presented as,

$$\mathbf{F} = \mathbf{\Gamma}(t)f_t.K_{cut} + \mathbf{\Psi}(t).K_{cut}.(\mathbf{x} - \mathbf{x}(t-T)) \tag{16}$$

$\mathbf{\Gamma}(t)$ and $\mathbf{\Psi}(t)$ are periodic functions with periodicity equal to the tooth passing period T. The forcing function consists of two components: a periodic component arising out of the feed force and a periodic regenerative component, coming from a periodic modulation of the chip thickness. The stability of the system is determined by the stability of the motions due to the regenerative component of the forcing function. Let $\mathbf{M}$, $\mathbf{C}$ and $\mathbf{K}$ be the generalized $m \times m$ mass matrix, damping matrix and stiffness matrices of the

structure. Assuming $\mathbf{x}$ to be the $m \times 1$ displacement vector, the dynamic equation of motion is given by,

$$\mathbf{M}\ddot{\mathbf{x}} + \mathbf{C}\dot{\mathbf{x}} + \mathbf{K}\mathbf{x} = \mathbf{b}\mathbf{F} \tag{17}$$

where b is the $m \times 2$ influence matrix containing the information about the degrees of freedom where the force vector $\mathbf{F}$ is acting. Substituting Equ. 16 in Equ. 17,

$$\mathbf{M}\ddot{\mathbf{x}} + \mathbf{C}\dot{\mathbf{x}} + \mathbf{K}\mathbf{x} - f_t.K_{cut}.\mathbf{b}\mathbf{\Gamma}(t) - K_{cut}.\mathbf{b}\mathbf{\Psi}(t).\mathbf{b}^T(\mathbf{x} - \mathbf{x}(t-T)) = 0 \tag{18}$$

In state-space notation, Equ. 18 can be written as,

$$\begin{Bmatrix} \dot{\mathbf{x}} \\ \ddot{\mathbf{x}} \end{Bmatrix} = \begin{bmatrix} \mathbf{0} & \mathbf{I} \\ -\mathbf{M}^{-1}\mathbf{K} & -\mathbf{M}^{-1}\mathbf{C} \end{bmatrix} \begin{Bmatrix} \mathbf{x} \\ \dot{\mathbf{x}} \end{Bmatrix} +$$

$$\begin{bmatrix} \mathbf{0} & \mathbf{0} \\ K_{cut}\mathbf{M}^{-1}\mathbf{b}\mathbf{\Psi}(t)\mathbf{b}^T & \mathbf{0} \end{bmatrix} \begin{Bmatrix} \mathbf{x} - \mathbf{x}(t-T) \\ \dot{\mathbf{x}} - \dot{\mathbf{x}}(t-T) \end{Bmatrix} + \begin{bmatrix} \mathbf{0} \\ K_{cut}\mathbf{M}^{-1}\mathbf{b}\mathbf{\Gamma}(t) \end{bmatrix} f_t \tag{19}$$

Equ. 19 represents a system of linear delay differential equation (DDE) with periodic coefficients. The solution for $\mathbf{x}$ consists of two parts: a periodic response due to the periodic feed force; the second part is due to the periodically modulated regenerative term, which decides the stability of the whole solution.

3 Stability Analysis

Chatter in milling is governed by delay differential equations with periodic coefficients. Two notable methods have recently been proposed for the analysis of such systems: the Temporal Finite Element Analysis method (Bayly et al. 2002; Mann et al. 2004) and the Semi Discretization method (Insperger et al. 2003b; Mann et al. 2003; Gradisek et al. 2005). Both methods apply the Floquet's theorem (Wiberg 1971) for stability analysis of periodic systems. The methods recognize the existence of multiple frequencies of chatter, as shown by Insperger, Mann, Stepan, and Bayly (2003a) and the occurrence of two kinds of instabilities, i.e., the Hopf and Flip Bifurcations. The instabilities are characterized by the peculiarity of the chatter frequencies.

- In case of Hopf Bifurcation, the chatter frequency is given by the expression $\omega_c = \pm\omega \pm \frac{2k\pi}{T}$, where $k = 0, 1, 2 \ldots$. Normally ω is approximately close to a modal fre-

quency of the structure and the other frequencies are separated from this frequency by harmonics of the tooth passing frequency.

- In case of Flip Bifurcation, the chatter frequencies occur at odd multiples of one half of the tooth passing frequency, i.e., $\omega_c = \pm\frac{\pi}{T} \pm \frac{2k\pi}{T}$. This form of instability does not happen in turning but may occur in low immersion milling operations.

Before the advent of these two methods, Minis (1993) had proposed the expansion of the periodic function $\mathbf{\Psi}(t)$ into a Fourier series and approximation of $\mathbf{\Psi}(t)$ with the zero-th order coefficient $\mathbf{\Psi_0}$. This makes the system time invariant. Altintas and Budak (1998) show that inclusion of some higher harmonics in the Fourier expansion do not give substantial differences in the stability limits for high immersion milling examples. This renders the zero-th order approximation sufficient for stability analysis of high immersion milling operations. Substituting $\mathbf{\Psi_0}$ for $\mathbf{\Psi}(t)$ and neglecting the feed term (assuming a linear analysis) and Laplace transforming Equ. 19 we get the following characteristic equation,

$$\det\left(s\mathbf{I} - \begin{bmatrix} \mathbf{0} & \mathbf{I} \\ -\mathbf{M}^{-1}\mathbf{K} + K_{cut}(1-e^{-sT})\mathbf{M}^{-1}\mathbf{b}\mathbf{\Psi_0}\mathbf{b}^T & -\mathbf{M}^{-1}\mathbf{C} \end{bmatrix}\right) = 0 \qquad (20)$$

Solving the characteristic equation for the chosen chatter frequency $s = j\omega_c$, the limiting K_{cut} and the the tooth passing period T can be obtained. This form of stability analysis is generally called the zero-th order single frequency solution for milling chatter. The method generates accurate stability limits for high immersion milling but cannot demonstrate the multiple chatter frequency perspective of chatter and does not identify the occurrence of Flip Bifurcations for low immersion milling, as shown in Bayly et al. (2002) and Insperger et al. (2003b). The reason is that the cutting process in low immersion milling is intermittent and the contribution of the high frequency harmonics of the Fourier expansion of $\mathbf{\Psi}$ may be substantial. Merdol and Altintas (2004) show that inclusion of the higher harmonics in the Fourier expansion of $\mathbf{\Psi}$, as proposed in Altintas and Budak (1998), can predict better stability limits for low immersion milling operations.

The complexities in the time varying nature of chatter in milling motivated the earlier researchers to study the phenomenon in time domain. Most of the work in this direction is done by Tlusty and his co-workers (1975, 1983, 1983). Tlusty and Ismail (1981) and Kondo and Sato (1981) incorporate the effect of the milling cutter, jumping out of the cut

and introduce the concept of the multiple regeneration process. A modified stability lobe diagram, involving the spindle speed, the peak to peak (PTP) magnitude of the cutting forces and the axial depth of cut is presented in Smith and Tlusty (1993). Smith and Tlusty (1990) observe the presence of a highly stable machining region in the stability lobe diagram for spindle speeds where the tooth passing frequency is approximately equal to a dominant modal frequency of the machine tool structure. Zhao et al. (Balachandran and Zhao 2001) show the occurrence of Flip and Hopf bifurcations and the existence of multiple chatter frequencies via time domain simulations for low immersion milling. The main drawback of a time domain simulation is that it is computationally inefficient. However, the inclusion of assumptions is minimal and the ability to incorporate various criteria make time domain simulations more realistic and a benchmark for comparing results from frequency domain analysis.

In the next sections, the development of the simulator for milling will be described and stability analysis will be performed, using the Root Locus Method with zero-th order approximation and time domain simulations. The results, obtained by these methods will be compared with experimental data and various aspects of milling chatter will be demonstrated.

4 Hardware in the Loop milling chatter simulator

Experimental characterization of chatter is difficult due to the involvement of a huge number of parameters and the requirement of numerous cutting tests. The characterization process requires the system to be actually unstable and this may be detrimental to the machine tool. The mathematical model of chatter is however, quite well-established. Representation of chatter as a feedback loop interaction between the structural dynamics and the cutting process is proposed by Merrit (1965) for turning, as shown in Figure 2. An alternative way to demonstrate chatter via a mechatronic simulator is proposed in this paper. The work follows the "Hardware in the Loop" concept, used for the development of a simulator for chatter in turning in the Active Structures Laboratory at ULB (Ganguli et al. 2005). The approach for milling is shown in Figure 6. Under the effect of the cutting forces, the flexible tool-workpiece system undergoes displacements. This along with the rotation of the tool creates the periodic regenerative effect and generate milling forces which further excite the machine tool structure.

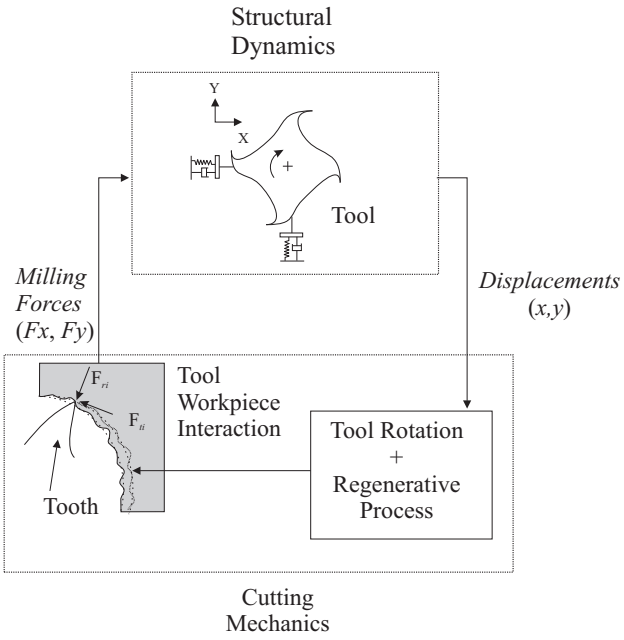

Figure 6: The dynamic milling model

The conceptual model of a 2 DOF simulator for milling is shown in Figure 7. The multi degree of freedom (MDOF) dynamics of the flexible machine tool and workpiece system is simulated by a rectangular hollow cantilever beam. Although it is understood that the machine tool structure is more complicated in terms of design and components, the dynamic behavior would be qualitatively same as the MDOF structural dynamics of a simple cantilever beam. Two voice coil actuators are attached to the free end of the beam in order to generate excitations in the two orthogonal directions. This simulates the cutting forces, acting on the cutting tool. The displacements in the two directions are sensed by eddy current sensors, manufactured by KAMAN Instrumentation and are fed into a DSP board, where a time domain simulation of the cutting forces is running. The dSpace Controldesk software provides a Graphical User Interface (GUI) to change the various cutting parameters, such as the axial width of cut, the spindle speed, the feed, the angles of entry and exit. The software calculates the system of cutting forces (calculated using Eqs. 14 and 15) according to the various cutting conditions, specified by the user. The calculated force signals are directed to current amplifiers through the output resources of the DSP board. The current amplifiers generate the necessary current to drive the voice coil actuators, according to the calculated cutting forces. For a chosen spindle

speed and cutting condition, a chatter situation can be triggered by gradual increase in the value of K_{cut}, until the oscillations of the beam start to grow. The cutting force or the displacement signals can be analyzed in a Fourier analyzer and the frequency content of the signal under stable and unstable conditions can be studied and conclusions can be made as to whether the instability is a Hopf or a Flip Bifurcation. This helps in characterization of the chatter instability in milling. The simulator also has an active damping setup, consisting of a couple of proof mass dampers also called Active Mass dampers (AMD) (manufactured by Micromega Dynamics S.A *www.micromega-dynamics.com*), collocated with accelerometers, located at an intermediate distance on the beam. Details of the control setup will be dealt with in a section devoted to active damping of chatter.

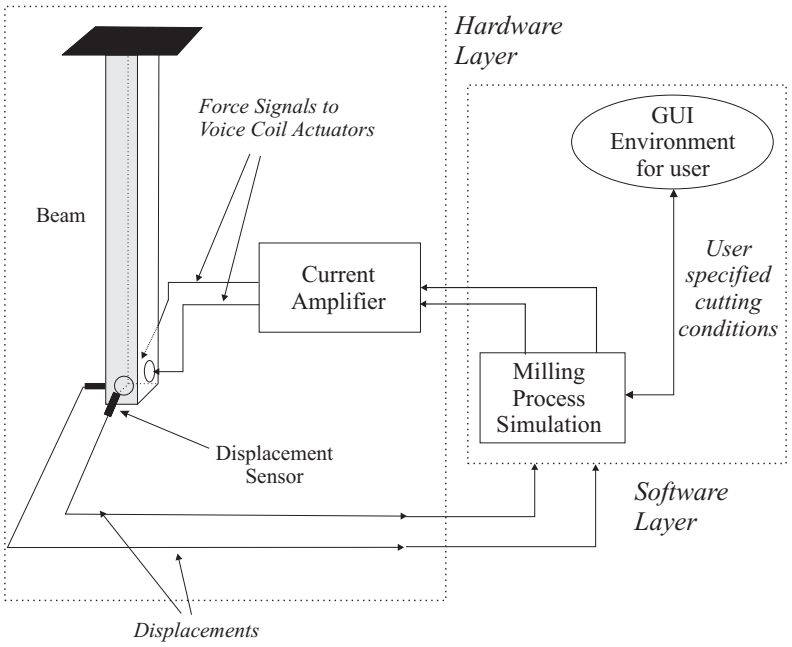

Figure 7: Conceptual model of the simulator for milling

4.1 Time domain simulations

Time domain simulations are performed to demonstrate the various aspects of chatter instability. For this purpose, a state space model of the mechanical setup is identified, using the MATLAB based Structural Dynamics Toolbox, developed by SDTools (SDTools). The identified frequency bandwidth is 100 Hz. The identified modal parameters are presented in the following table.

Modes	Frequency (Hz)	Damping (%)
Active Mass Damper X direction	8	20
Active Mass Damper Y direction	8.9	14
1st Flexible Mode X direction	37	2
2nd Flexible Mode X direction	66.9	1
1st Flexible Mode Y direction	60.6	1.1
2nd Flexible Mode Y direction	72.8	0.9

Table 1: Modal frequencies and damping properties of the beam-PMD setup

In comparison to the natural frequencies of a real machine tool, where the tool modes are normally hundreds or thousands of Hz, the modal frequencies of the beam are rather low. However, within the framework of the SMARTOOL project (*www.smartool.org*) under which the work was performed, there were real machining centers with chattering modes within 50 and 100 Hz. This guided the choice of the natural frequency of the first mode of the beam. The time domain simulations were performed via a SIMULINK model that utilizes the identified state-space model of the beam and simulates the regenerative cutting process to calculate the cutting forces, according to the formulae (Eqs. 14 and 15) in Section 2.

The time domain simulation for a milling example is performed with the following cutting parameters: 50 % immersion upmilling, i.e., angle of cut is 90 degrees, feed $f_t = 0.1$ mm per revolution, spindle speed $N = 1200$ RPM, number of teeth $n = 4$. A low value of K_{cut} is chosen to demonstrate a stable machining situation at this spindle speed. The power spectral density (PSD) of the cutting force signals in the **X** and **Y** directions at this spindle speed are shown in Figure 8. Both of the spectra is dominated by the tooth passing frequency at 80 Hz (calculated as Spindle Speed $\times$ Number of Teeth/60) and its harmonics.

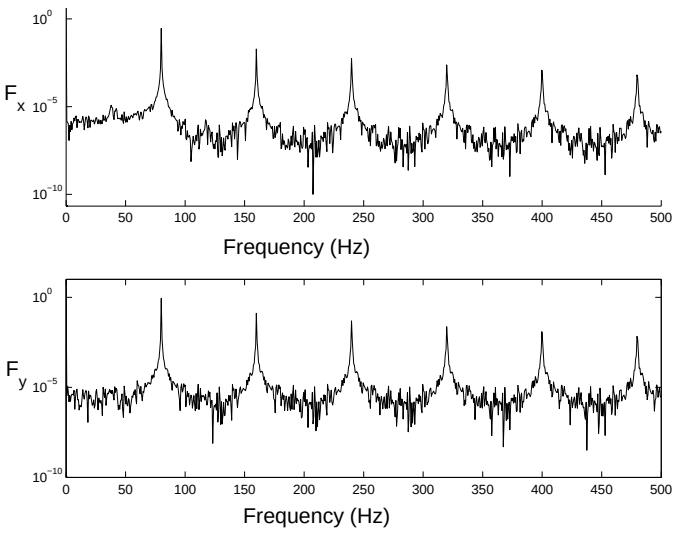

Figure 8: PSD of the cutting forces at 1200 RPM under a stable condition

The spectra of the displacements in the two directions are shown in Figure 9. The tooth passing frequencies are marked by circles. The signal in the **X** direction contains the first flexible modal frequency at approximately 37 Hz, the second flexible mode at 66 Hz and the harmonics of the tooth passing frequency. For the **Y** direction, the two modal frequencies are visible, with the second bending mode more dominant, due to its proximity to the excitation tooth passing harmonic.

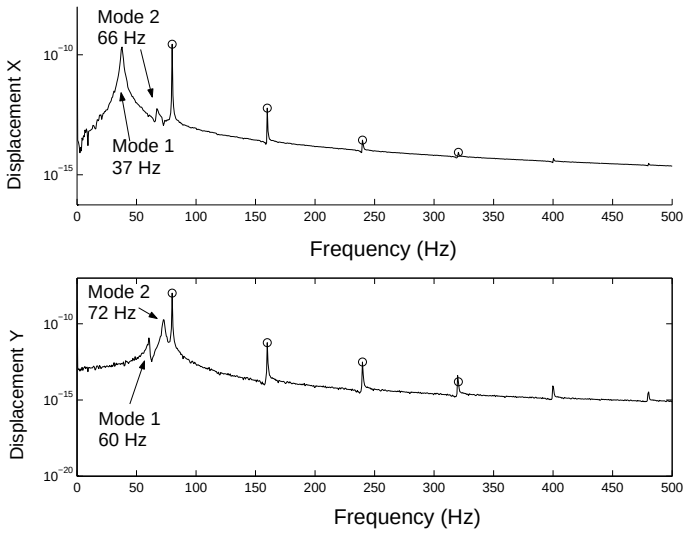

Figure 9: PSD of the displacements in a stable cutting condition at 1200 RPM

Unstable and stable situations are compared for a spindle speed of 1500 RPM and varying cutting conditions. The PSD of the displacement signals for unstable situations are presented with continuous lines and those corresponding to stable situations are presented with dotted lines. In an unstable situation, several peaks appear in the PSD plot. Some of the peaks correspond to the harmonics of the tooth passing frequency and the others to the chatter frequencies. The separation between two successive chatter frequencies is equal to the tooth passing frequency. In Figure 10, a chatter situation for slotting (180 degrees angle of cut) with the 4 teeth tool, described before, is investigated for 1500 RPM. The PSD of the displacements show only a single frequency and no tooth passing frequency. This can be explained as follows. For slotting with four teeth, there will always be two teeth in contact with the workpiece and the remaining teeth will be out of the cut. The angle between successive teeth is 90 degrees. Due to this orientation of the teeth inside the cut, it can be shown from Equ. 14 and 15, that the feed force and the milling force coefficients are always constant for any location of the teeth inside the cut. Therefore slotting is a special case in milling, where the milling coefficients remain constant and there is no periodicity in the feed forces and the regenerative process. Therefore, unlike in Figure 9, the tooth passing frequencies are absent in the displacement spectra. The instability is similar to the case of turning since there is only one chatter frequency. The same chatter frequency arises in the two directions, since there is a coupling between

the two directions through the milling coefficient matrix $\mathbf{\Psi}$. There may also be some mechanical coupling between the two directions since the placement of the actuators may not be exactly on the vertical middle line of the beam. So if there is some vibration at a particular frequency in one direction, it excites the other direction as well at the same frequency. In Figure 11, a chatter condition for 50% upmilling at 1500 RPM with

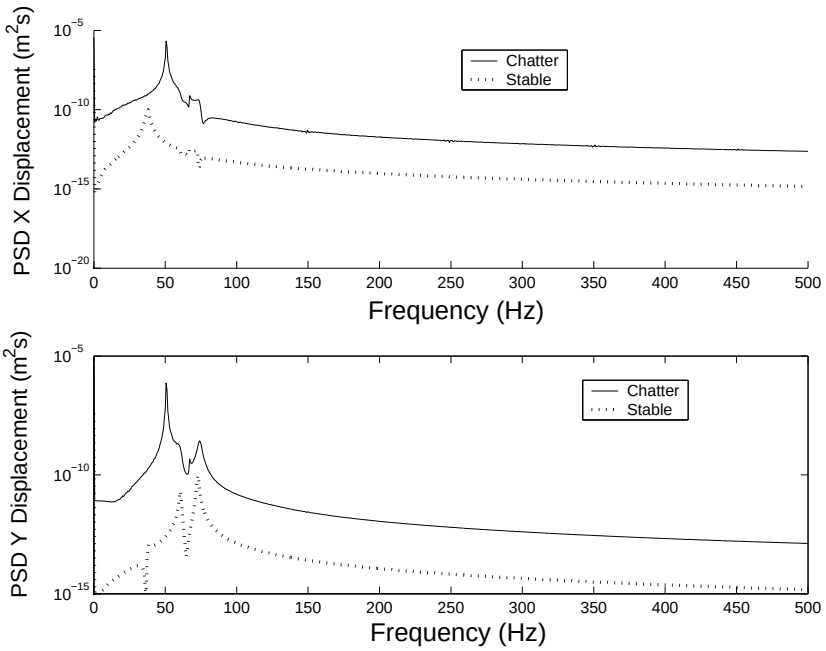

Figure 10: PSD of displacements for slotting at 1500 RPM

4 teeth is investigated. The tooth passing frequency at multiples of 100 Hz are marked by circles. The case is that of a Flip Bifurcation since the chatter frequencies (marked by black squares) exist at multiples of one half of the tooth passing frequency of 100 Hz.

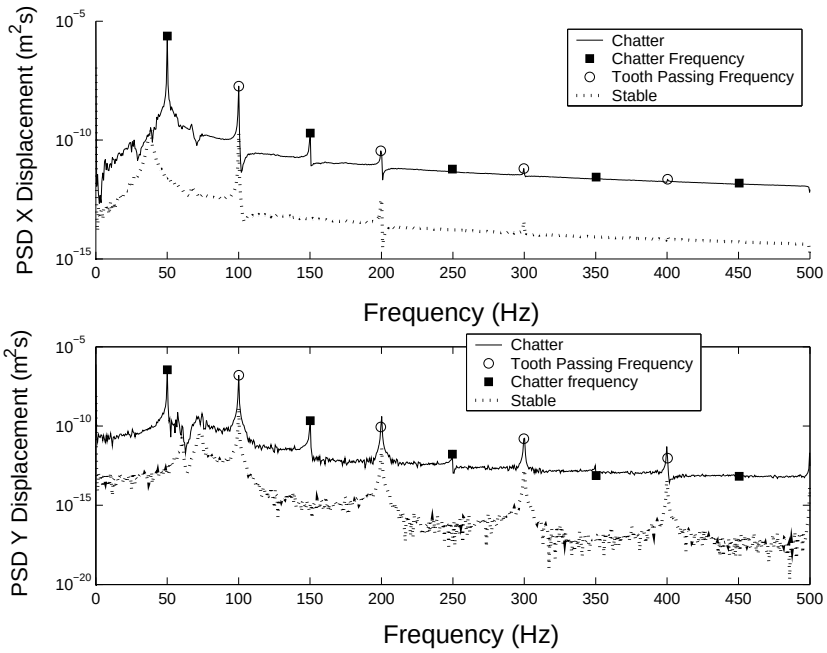

Figure 11: PSD of displacements for 50% immersion upmilling at 1500 RPM

For 50% immersion downmilling for the same spindle speed, the case is that of a Hopf Bifurcation, as shown in Figure 12. The dominant chatter frequency arises from the second flexible mode in the $\mathbf{Y}$ direction at 72 Hz. The chatter frequency is not commensurate with the tooth passing frequency at 100 Hz, which is normal for Hopf Bifurcation. A low immersion upmilling example, with an angle of cut equal to 30 degrees, is examined in Figure 13. The instability is Flip Bifurcation since the chatter frequencies are at integer multiples of one half of the tooth passing frequency. A popular way of identifying whether an instability is Hopf or Flip Bifurcation is by sampling the displacement signal, once per tooth passing period. The procedure is proposed by Scmitz (Schmitz 2003) for chatter recognition by sensing the sound signal, generated in the cutting process. The technique has been used for detecting the type of instability by many authors in subsequent works. If during a Flip Bifurcation, the basic chatter frequency is 50 Hz and the tooth passing frequency is 100 Hz, a one per tooth pass sampling will generate 2 samples of displacement, during one period of oscillation of the structure. At the stability limit, assuming that the displacement neither grows or decays and the system oscillates with a single dominant frequency, the sampled signal value will always have two exact values. This is shown in

Figure 14 a) for the low immersion milling example at 1500 RPM. This characteristic of the sample displacement signal helps to identify a Flip Bifurcation situation. In case of Hopf Bifurcation, there is no relationship between the basic chatter frequency and the tooth passing frequency. So sampling once per tooth passing period will not yield any particular characteristic of the distribution of the data with time, as in the case of Flip Bifurcation. A Hopf Bifurcation case for 50% immersion downmilling is shown in Figure 14 b).

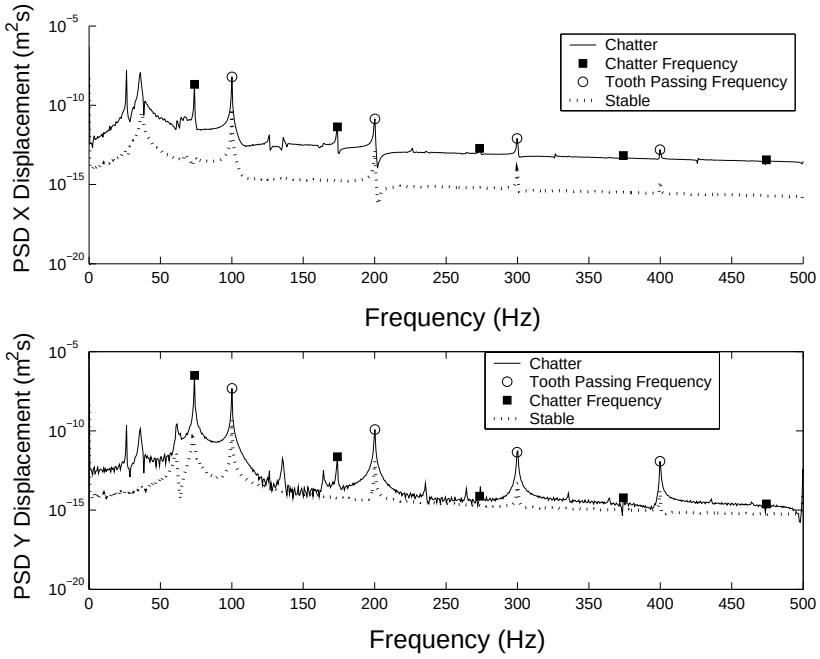

Figure 12: PSD of displacements for 50% immersion downmilling at 1500 RPM

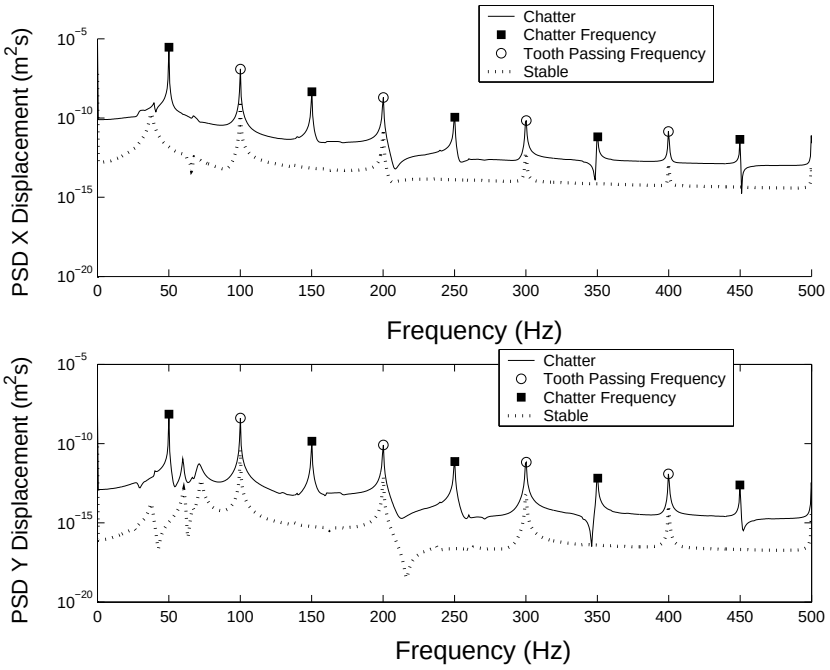

Figure 13: PSD of displacements for low immersion upmilling at 1500 RPM

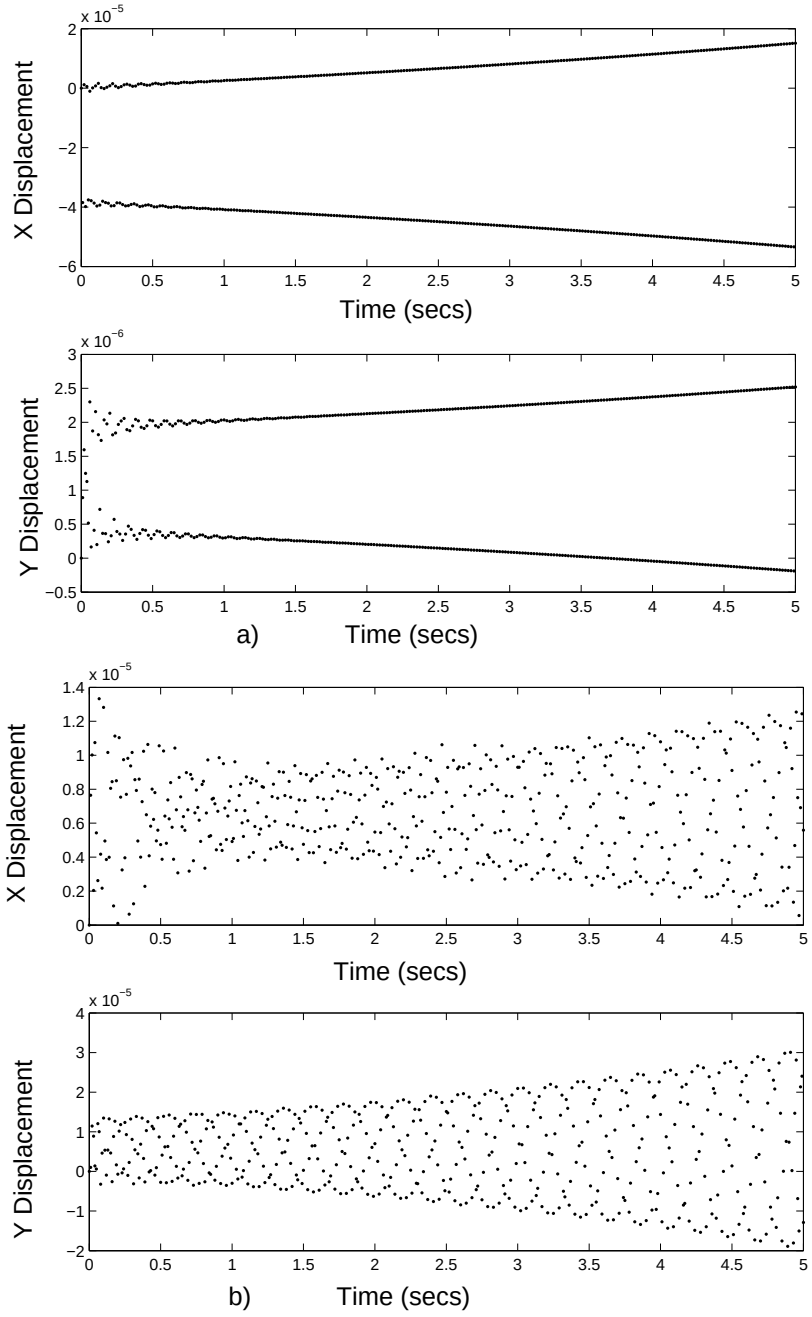

Figure 14: Demonstration of once per revolution sampled data for a) Flip Bifurcation b) Hopf Bifurcation

4.2 Stability Limits

Stability limits, obtained by time domain simulations are compared with the results obtained by the Root Locus Method. Two approximations are made in the Root Locus Method. The 2 DOF system has two delay terms instead of one to simulate the regeneration terms for the two directions. They are approximated by the Padé Approximation for eigenvalue analysis, as described in Ganguli et al. (2005). The periodic term $\mathbf{\Psi}$ is approximated by the constant matrix $\mathbf{\Psi_0}$. This transforms the problem to a DDE with constant coefficients. For a chosen spindle speed and increasing values of K_{cut}, the eigenvalue problem for the system is solved. The value of K_{cut}, corresponding to which a couple of conjugate roots cross the imaginary axis is taken as the stability limit for that spindle speed. Figure 15 shows the evolution of the roots of the closed loop system in the complex plane. Since the system is described by a transcendental DDE, along with the structural poles, there are infinite number of eigenvalues, corresponding to the delay. The Padé approximation converts the system to one with finite number of roots by approximating the delay term by a rational fraction in s. As shown in Figure 15, the eigenvalues of the system migrate towards the imaginary axis with increasing K_{cut}. The value of K_{cut}, for which a pair of conjugate roots are on the imaginary axis, is the stability limit. The stability lobe diagram is constructed by plotting the ratio between limiting K_{cut} and

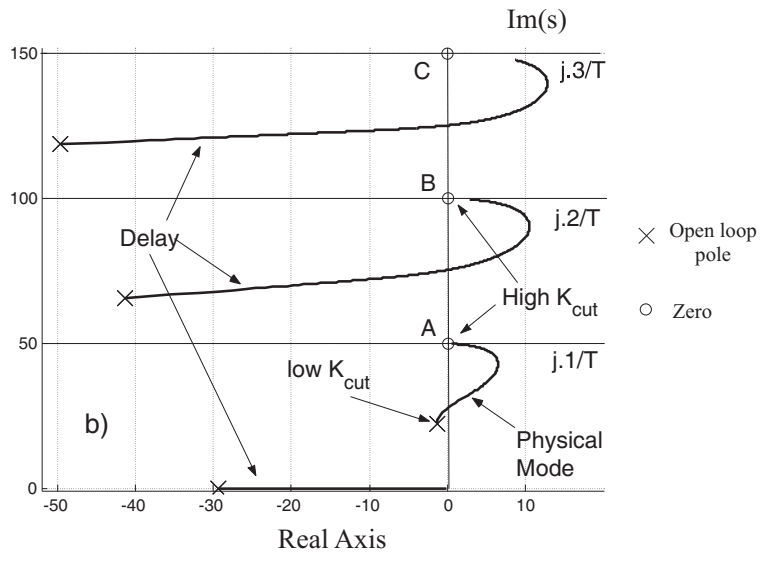

Figure 15: Evolution of eigenvalues with increasing K_{cut}

structural stiffness in the **X** direction, for various spindle speeds. Numerical simulations

are performed for 4 cases of milling operations with a 4 teeth tool : slotting , 50% immersion up and downmilling and a case of low immersion upmilling with angle of cut equal to 30 degrees. Figure 16, shows the results for slotting. The time domain and the Root Locus simulation results are exactly on top of each other. A high stability region is located between 400 and 600 RPM. The spindle speed corresponding to the highest value of the stability limit, obtained experimentally, is 535 RPM. The tooth passing frequency at this spindle speed is approximately equal to 36 Hz, which is near the first bending mode in the more flexible **X** direction.

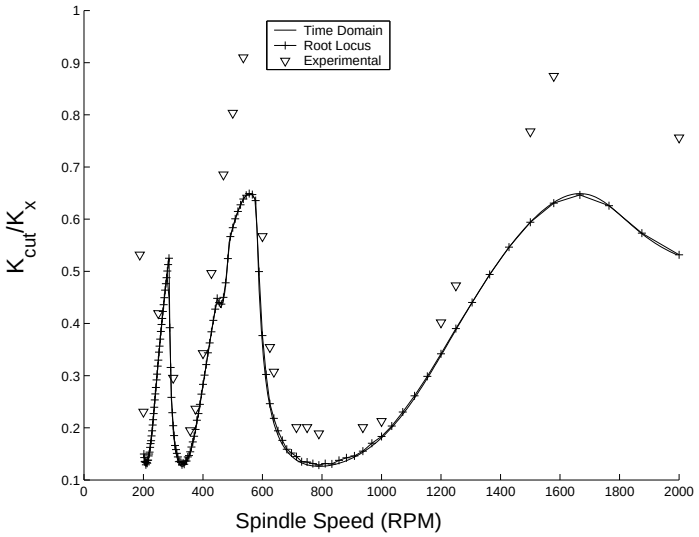

Figure 16: Comparison between stability limits obtained experimentally, by the Root Locus Method and by Time domain simulations for a slotting operation

In figures 17 a) and b), the stability limits corresponding to 50% upmilling and downmilling are plotted. For upmilling, the Root Locus method gives a good match at spindle speeds lower than 1000 RPM. Certain portions of the stability lobe diagram, where Hopf and Flip Bifurcations occur are identified by the oval shaped regions in the Figure 17 a). The stability limits, obtained by the Root Locus Method for the Flip Bifurcation regions do not match with their counterparts from the time domain simulation results. In Figure 17 b), the Root Locus results do not show the Flip Bifurcation regions. In Figure 18, a study of a low immersion milling example with angle of cut equal to 30 degrees is presented. The stability lobes obtained from time domain simulations show a prominent

region, where Flip Bifurcation is occurring, which is not observed in the Root Locus result.

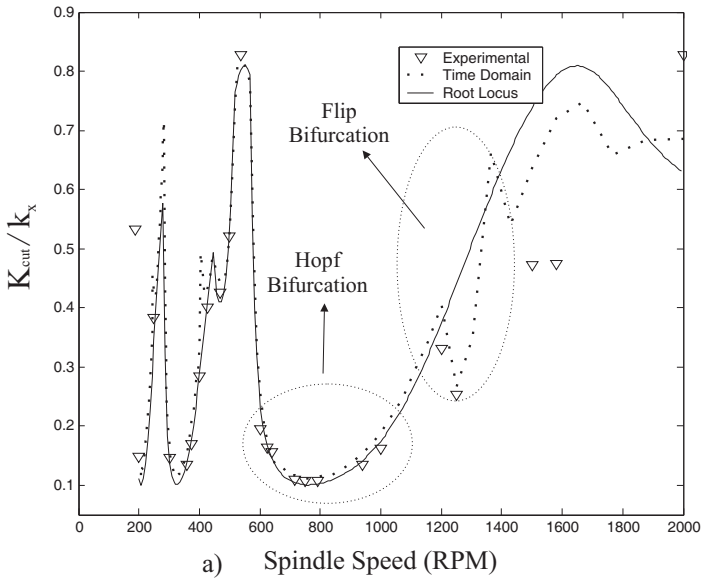

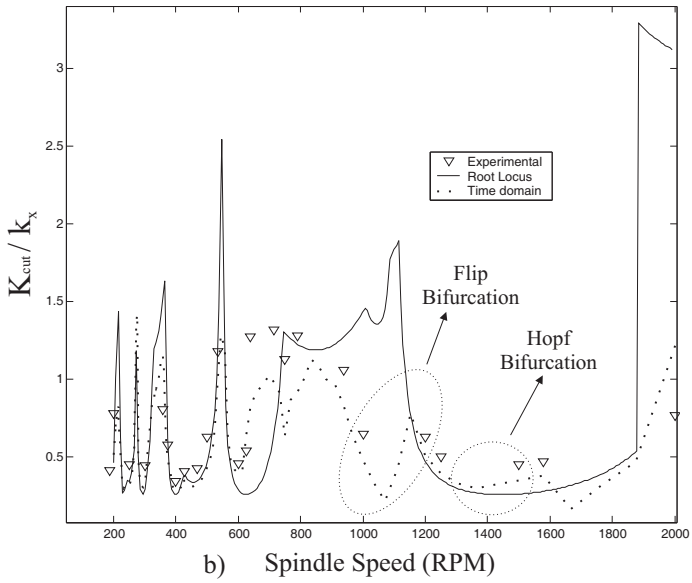

Figure 17: Comparison between stability limits obtained experimentally, by the Root Locus Method and by Time domain simulations for 50% immersion a) upmilling and b) downmilling

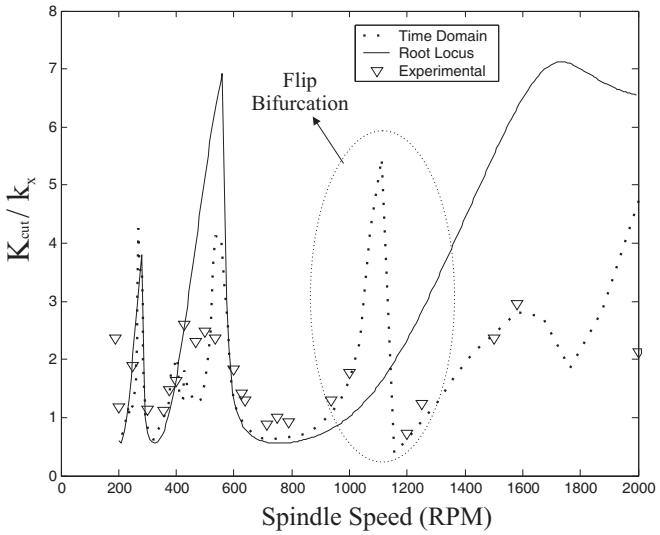

Figure 18: Comparison between stability limits obtained experimentally, by the Root Locus Method and by Time domain simulations for low immersion milling

4.3 Experimental Results

Stability analysis is performed on the setup experimentally and the stability limits for different milling operations are plotted in Figures 16, 17 and 18 for comparison with numerical results. For a chosen spindle speed, K_{cut} is increased stepwise until the onset of unstable oscillations, which are monitored on a PC. The corresponding value of K_{cut} is stored as the stability limit for the chosen spindle speed. In case of slotting, as shown in Figure 16, the experimental results follow the results from time domain simulation and the Root Locus analysis technique. For upmilling, experimental results match very well with numerical results for spindle speeds less than 1000 RPM. The experimental results deviate from the numerical results, especially from the Root Locus results in the Flip bifurcation regions at high spindle speeds. In the case of downmilling, the experimental results follow the time domain simulation data but are not in good agreement with the results from the Root Locus method. For low immersion upmilling in Figure 18, the experimental data match very well with time domain results. Figures 19 a) and b) represent the experimental PSD of the displacement in the **X** direction for a low immersion milling operation. A Hopf bifurcation scenario occurs for 750 RPM and a Flip bifurcation occurs for 1200 RPM.

The results of the numerical and experimental investigations can be summarized as

follows. The experimental stability lobes follow the same trend as the time domain simulation results for all the milling examples. The Root Locus Method has good agreement with the time domain and experimental results for high immersion milling. For partial immersion milling, there is agreement in the Hopf Bifurcation regions of the stability lobe diagram but the match is not good for spindle speeds where Flip Bifurcations occur.

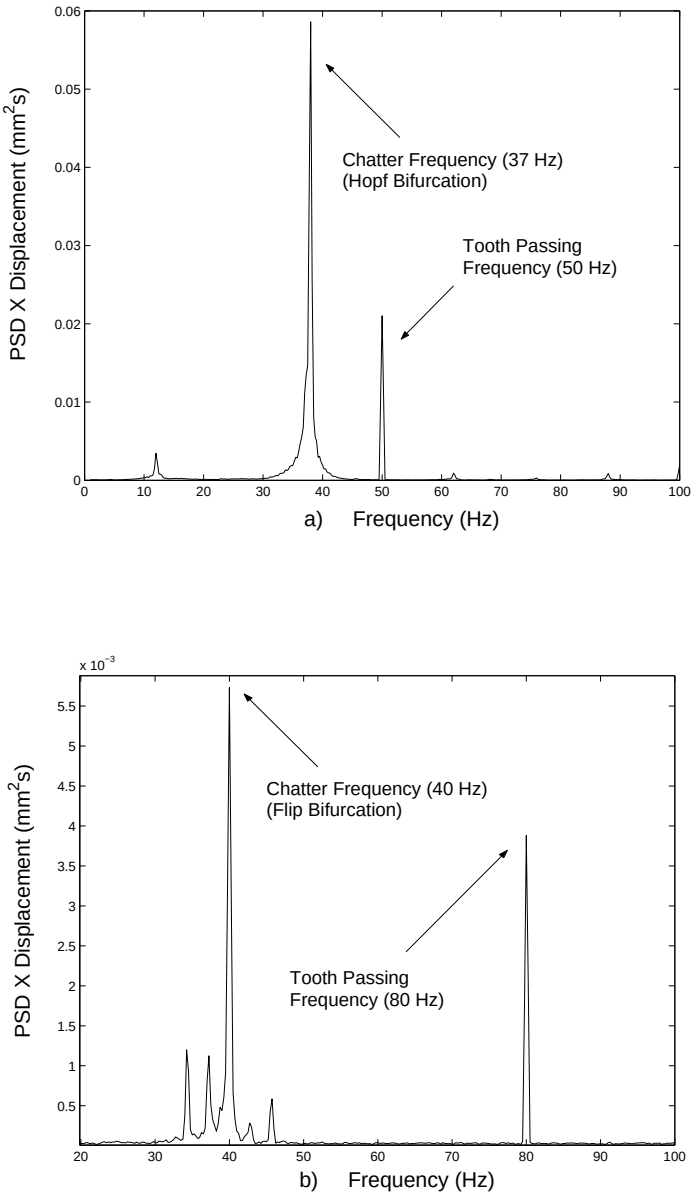

Figure 19: Experimental demonstration of a) Hopf bifurcation (750 RPM) and b) Flip bifurcation (1200 RPM)

5 Application of active damping for chatter control

Control of chatter is an important subject of research. The stability lobe diagram (Tobias and Fishwick 1958a; Tobias and Fishwick 1958b) is the first attempt to avoid chatter instability during a machining process. Efforts have been made by Slavicek (1965) to avoid chatter by changing the geometry of the tool. Among the active control techniques of chatter, the spindle speed modulation technique and the spindle speed selection techniques are quite popular. The spindle speed modulation technique involves periodic variation of the spindle speed with very low frequency, as proposed by Hoshi et al. (1977) experimentally and also by Sexton et al. (1978) and Lin et al. (1990). However, the modulation technique is costly and limited by the inertia of the rotating parts of the machine. Smith and Tlusty (1992), present a spindle speed selection technique, which iteratively finds out the spindle speed, corresponding to the maximum stability region in the stability lobe diagram. Soliman and Ismail (1998) present a control system that ramps up the spindle speed until a stable machining situation is reached.

Vibration control strategies have also been attempted for chatter control. In many studies on chatter, it has been observed that machining stability can be enhanced by increased damping of the whole system. Tlusty (1978) shows that damping in the cutting process stabilizes chatter. Merrit (1965) shows that increase in the structural damping would raise the asymptotic threshold of stability and the region of stable machining would increase. Passive damping techniques such as the "Lanchester" damper have been proposed in Hahn (1951), impact dampers in Ema and Marui (2000) and tuned mass dampers in Tarng, Kao, and Lee (2000). But the amount of damping achievable is limited and the performance of tuned mass dampers depends on the accurate tuning between the damper frequency and the structural modal frequency. Active vibration control strategies have also been applied for chatter control. Glaser et al. (1979) and Nachtigal (1972) propose a feedforward strategy of using the cutting force signal for chatter control in turning. An adaptive control technique, using filtered-X least mean square algorithm is proposed by Browning, Golioto, and Thompson (1997) for chatter suppression in boring bars. Dohner et al. (2004) propose a pole placement strategy using a LQG controller and strain gage sensors and electrostrictive actuators for milling. Smart fluids such as electrorheological or magnetorheological fluids have been used for chatter suppression in Segalman and Redmond (1996).

In the present work, an active damping strategy using a collocated sensor actuator configuration is used for chatter control on the simulator. Active damping for chatter suppression in milling have been applied by Chung et al. (1997) and more recently by Sims et al. (2003), (2005). In the latter case, the authors have used collocated piezoelectric sensor and actuator patches on thin flexible workpieces to actively damp chatter vibrations. A collocated configuration ensures unconditional stability in the closed loop (Miu 1991; Preumont 2002). However, the present setup is not strictly collocated, as will be shown in a later part of this section.

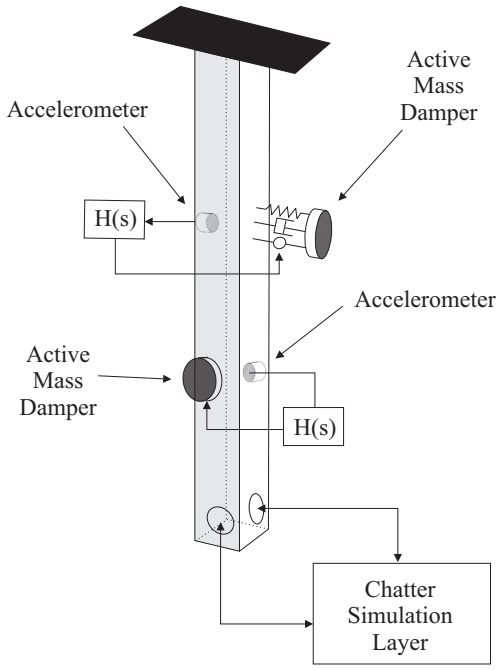

Figure 20: Active damping setup for the 2 DOF simulator

Certain structural modifications are made on the simulator setup. Two retroreflectors are mounted at the tip of the beam in the two directions as part of a ZYGO laser interferometry setup, used to measure the displacements in the two directions. The modal properties of the setup are thus changed (shown in Table 2). Active damping is applied in the two directions by two decentralized local acceleration feedback loops. The setup, as shown in Figure 20, consists of two AMDs, collocated with a pair of accelerometers, which sense the acceleration signal in the two directions. These signals are fed into the controllers, shown by $H(s)$, integrated and multiplied by a gain and fed into the AMDs.

A similar approach, using inertial actuators, is adopted by Cowley (1970). The simulator now has two independent layers: the chatter simulation loop and the active damping loop. A photograph of the whole setup is shown in Figure 21.

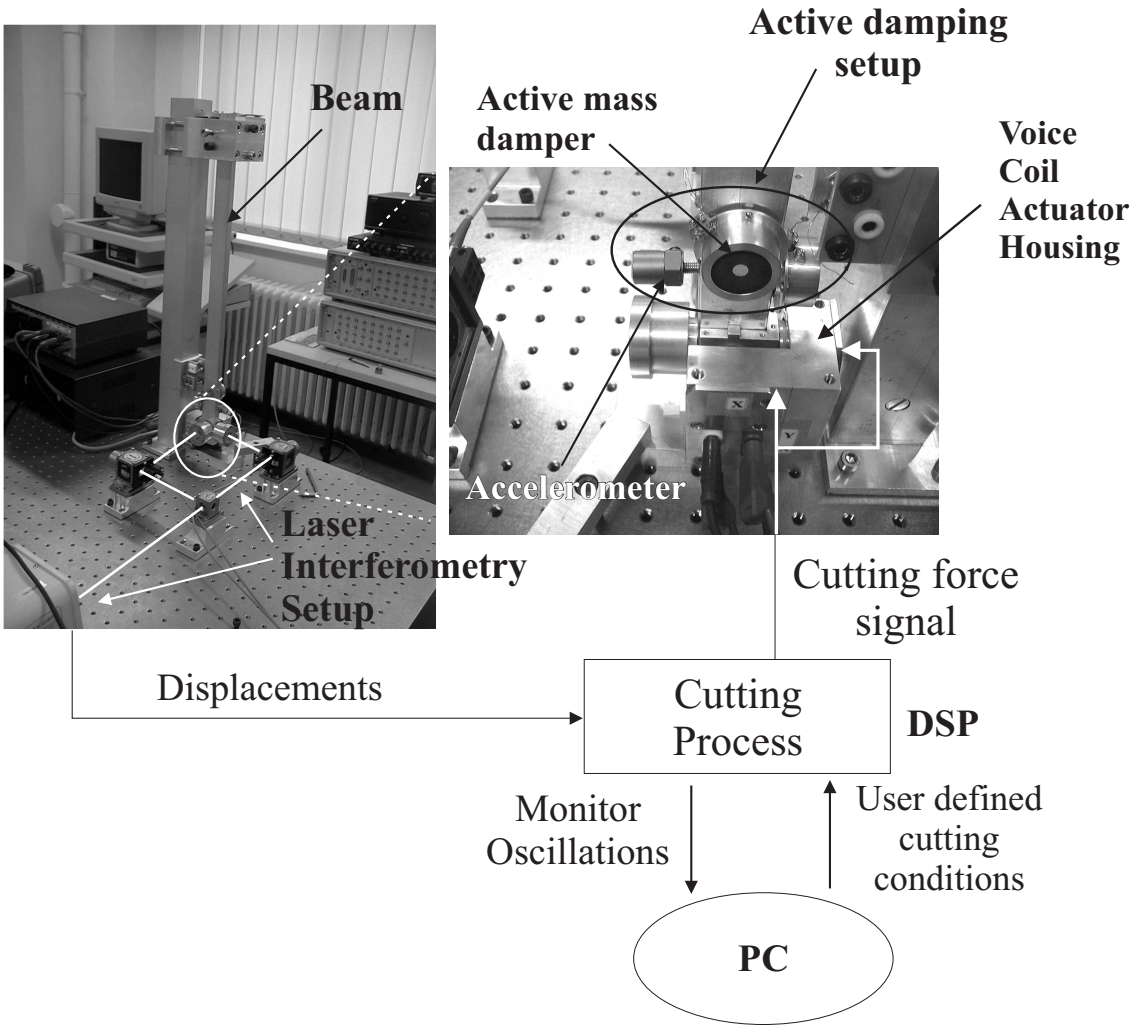

Figure 21: The experimental setup

Mode	Uncontrolled		Controlled 1		Controlled 2	
	ω (Hz)	ξ (%)	ω (Hz)	ξ (%)	ω (Hz)	ξ (%)
Bending X	25.7	2.1	25.1	6.7	24.3	8.2
Bending Y	48.1	2.7	46.2	4.5	46.2	5.8
Torsion	67.6	0.8	67.8	0.8	67.6	0.5

Table 2: Modal frequencies and damping properties of the beam−AMD setup

Two feedback gains are applied in each active damping loop and the structural properties with and without control are compared in Table 2. The case corresponding to "Controlled 2" has higher feedback gains in comparison to "Controlled 1" case. It is observed that higher feedback gains augment damping in both of the bending modes in the two directions. This is demonstrated by Root Locus plots in Figure 22 a) and b). It can be commented that the control setup is not an exact collocated system since the feedback signal is the absolute acceleration of the beam at the location of the sensor and the control force is a relative electromagnetic force between the beam and the proof mass. However, the arrangement is the closest approximation of collocated feedback control, achievable in the present setup. Thus, an alternate pole zero configuration of a collocated system is not observed in the Root Locus plots. In Figure 22 a), the actuator mode becomes unstable and the maximum damping ratio achievable in the first bending mode is about 50%. In the **Y** direction, the control system is able to apply critical damping to the system. However, experimentally such high damping ratios were not achievable. No particular reason was found to be responsible for the low closed loop damping values, since several factors, such as spillover effect from the high frequency modes, finite bandwidth of the electronic hardware may be lead to an unstable closed loop. Thus the maximum achievable damping, 8.2% for **X** and 5.8% for the **Y** direction, are lower than the theoretical values for both directions.

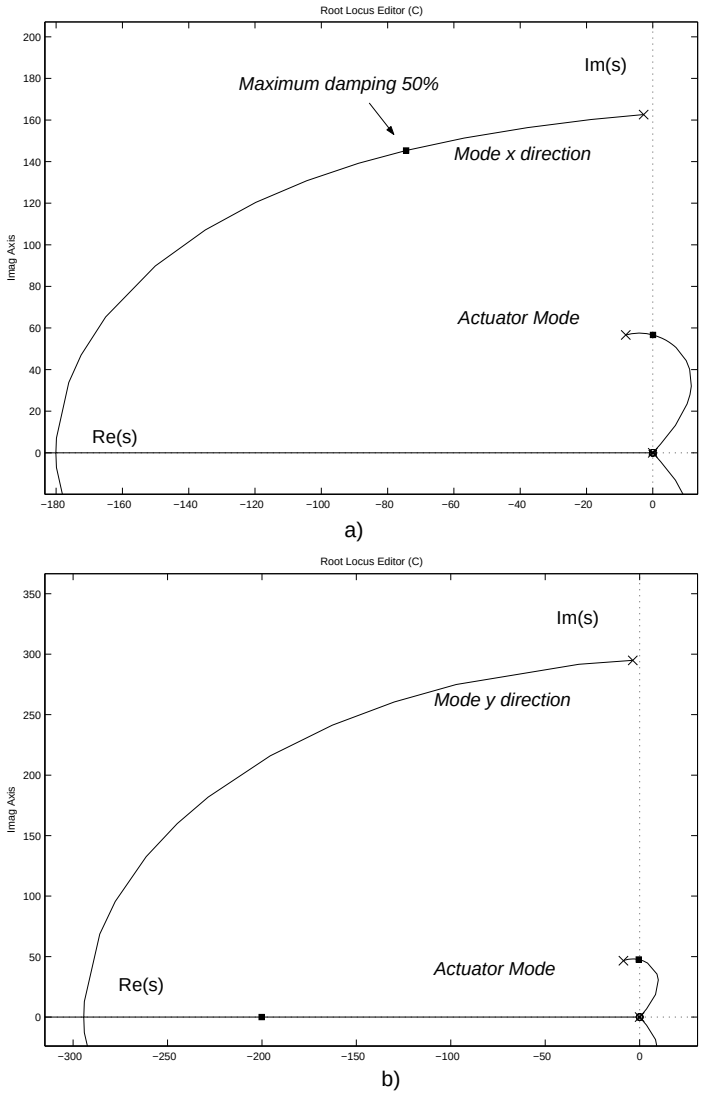

Figure 22: Loci of closed loop poles due to active damping a) **X** direction b) **Y** direction

The effect of active damping on the stability of slotting, upmilling and downmilling is investigated numerically and experimentally. Figures 23 a) and 24 a) compare the numerical and the experimental data for the undamped system and the two controlled cases for slotting and upmilling respectively. The experimental data follow the time domain simulation results quite well. The experimental results in Figures 23 b) and 24 b) show a general rise in the stability lobe diagrams, especially in the low stability regions.

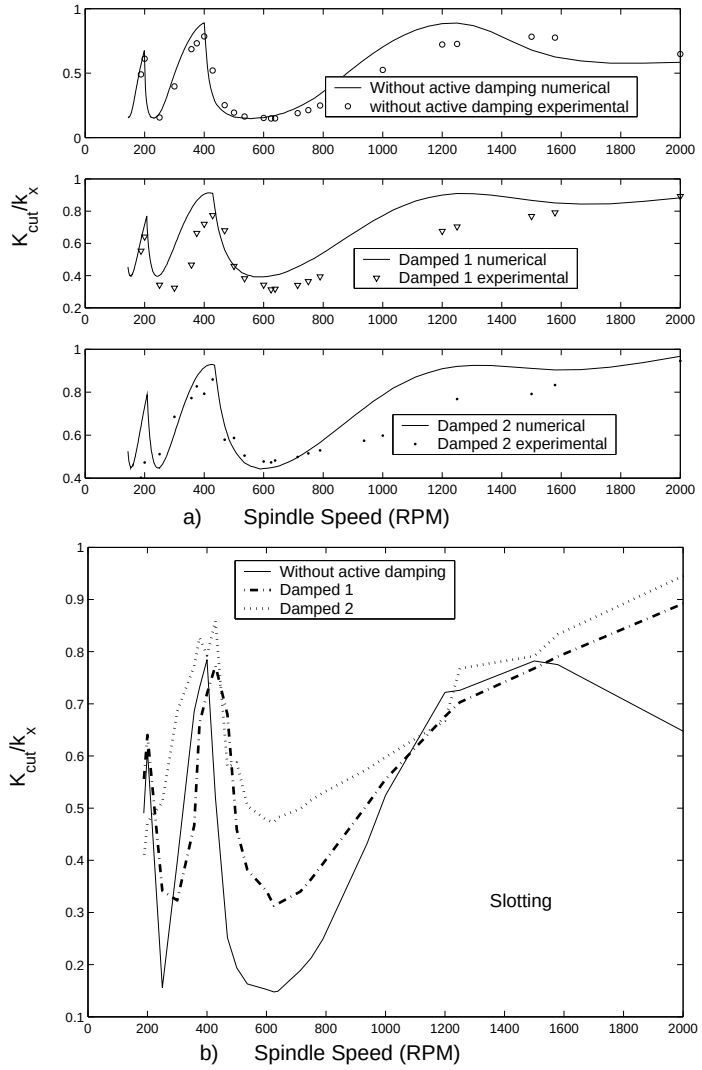

Figure 23: Comparison between a) numerical and experimental stability lobes b) experimental stability lobes for slotting with and without active damping

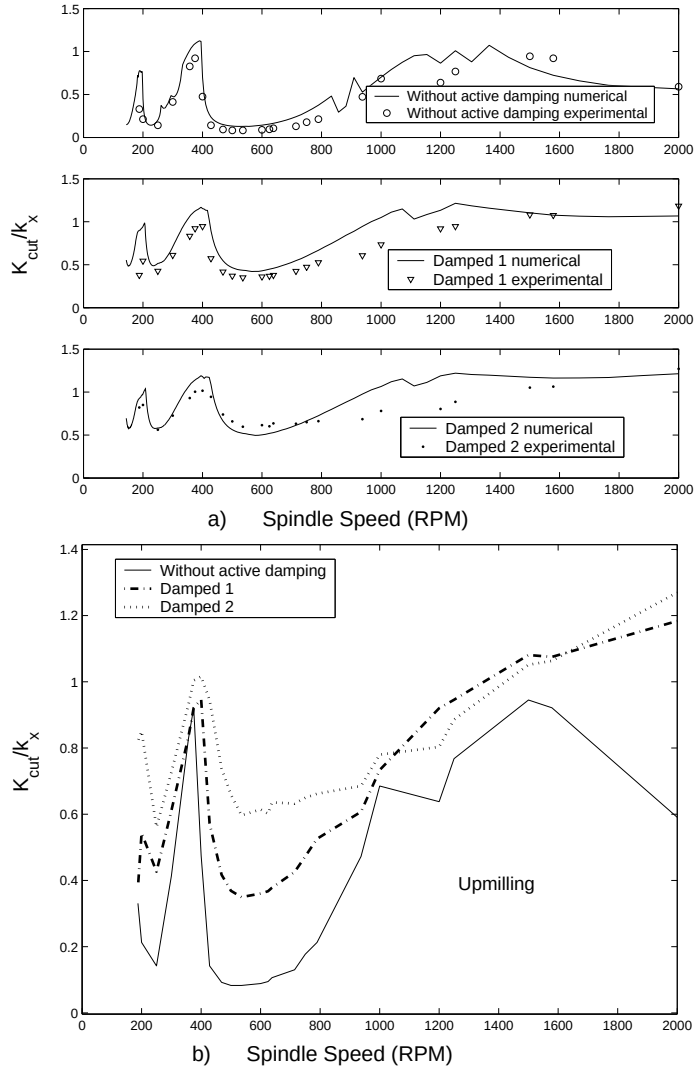

Figure 24: Comparison between a) numerical and experimental stability lobes b) experimental stability lobes for upmilling with and without active damping

In case of downmilling, as shown in Figure 25 a), the match between the experimental and the numerical results is not very good and the authors could not explain the fall in the level of stability at certain spindle speeds for the higher value of feedback gain. However, Figure 25 b) still shows that active damping is able to raise the stability limits.

Therefore, the active damping technique seems to be an efficient strategy for stabilizing chatter in milling, just as in the case of turning (Ganguli et al. 2005). It is observed that active damping is more efficient in enhancing the stability in the low stability regions than

the high ones. This can be seen as an advantage of active damping over spindle speed selection technique of chatter control (Smith and Tlusty 1992). The latter normally changes the spindle speed iteratively to the highest stability region of the stability lobe diagram and allows one to machine with high values of axial width of cut. However, the stability lobe diagram tapers in the high stability regions and a change in system dynamics may shift the lobes horizontally, leading to instability in a previously stable situation. Low stability regions are less susceptible to changes in system dynamics. Application of active damping raises these low stability regions, enabling one to machine with higher values of axial depth of cut in a region, less vulnerable to changes in the system dynamics.

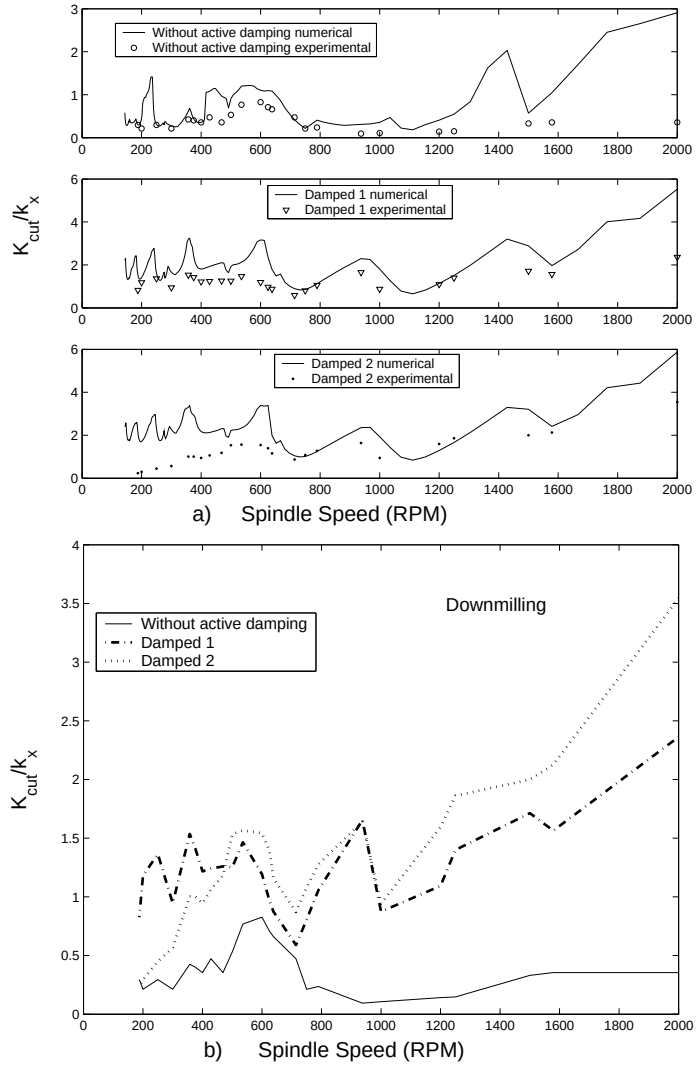

Figure 25: Comparison between a) numerical and experimental stability lobes b) experimental stability lobes for downmilling with and without active damping

6 Conclusion

The paper presents a 2 DOF mechatronic simulator for the study of chatter in the milling process. The simulator follows the regenerative milling process model and can experimentally simulate the occurrence of Hopf and Flip bifurcations in various kinds of milling operations. The experimental stability lobes are found to match well with the numerical time domain results. This shows the capability of the simulator to simulate regenerative

chatter in milling realistically.

Active damping, as a chatter control strategy is also implemented in the setup. It is shown that active damping is able to stabilize all kinds of milling operations by raising the stability limits. The effect is more pronounced in the low stability regions of the stability lobe diagram of the uncontrolled system than the originally high stability regions. This can be seen as an advantage of active damping over spindle speed selection technique of chatter control. Thus, active damping can be proposed as a potential candidate for stabilization of chatter in real machining operations.

The simulator has some limitations in terms of the maximum spindle speeds it can simulate due to bandwidth limitations of the hardware, i.e., the displacement sensor, the actuator and the amplifiers used in the experimental investigations and the computational resource. However, if viewed from a qualitative perspective, spindle speed frequencies higher than the dominant natural frequency of the structure can be viewed as high spindle speeds. The simulator is able to simulate cutting at 2000 RPM with 4 teeth. The corresponding tooth passing frequency is about 5 times the first modal frequency of the structure and therefore the chosen range of spindle speed considers a high spindle speed part. The paper presents a qualitative study of regenerative chatter in milling and the associated mechanisms of instability via a mechatronic simulator. The potential of active damping for chatter reduction is also demonstrated in the setup. The simulator thus fulfills an intermediate step between theory and actual implementation of active damping on a real setup in the framework of the SMARTOOL project.

7 Acknowledgement

The authors wish to thank the SMARTOOL Consortium and the European Commission for funding the project (Contract No. GIRD-CT-2001-00551). The authors also thank the Inter University Attraction Pole (IUAP S-06,AMS) programme between Belgian Universities.

References

Altintas, Y. (2000). *Manufacturing Automation*. Cambridge University Press.

Altintas, Y. and E. Budak (1998). Analytical prediction of chatter stability in milling -

part 1: Application of the general formulation to common milling systems. *Journal of Dynamic Systems, Measurement and Control, Transactions of the ASME 120*, 23–30.

Balachandran, B. and M. X. Zhao (2001). Dynamics and stability of milling process. *International Journal of Solids and Structures 38*, 2233–2248.

Bayly, P. V., B. P. Mann, T. L. Schmitz, D. A. Peters, G. Stepan, and T. Insperger (2002). Effects of radial immersion and cutting direction on chatter instability in end-milling. *Proceedings of IMECE 2002, ASME International Mechanical Engineering Congress and Exposition*.

Browning, D. R., I. Golioto, and N. B. Thompson (1997). Active chatter control system for long-overhang boring bars. *Proceedings of the SPIE 3044*, 270–280.

Chung, B., S. Smith, and J. Tlusty (1997). Active damping of structural modes in high speed machine tools. *Journal of Vibration and Control 3*(3), 279–295.

Cowley, A. Boyle, A. (1970). Active dampers for machine tools. *Annals of the CIRP 18*, 213–222.

Dohner, J. L., J. P. Lauffer, T. D. Hinnerichs, N. Shankar, M. Regelbrugge, C. Kwan, R. Xu, B. Winterbauer, and K. Bridger (2004). Mitigation of chatter instabilities in milling by active structural control. *Journal of Sound and Vibration 269*, 197–211.

Ema, S. and E. Marui (2000). Suppression of chatter vibration of boring tools using impact dampers. *International Journal of Machine Tools and Manufacture 40*, 1141–1156.

Ganguli, A., A. Deraemaeker, M. Horodinca, and A. Preumont (2005). Active damping of chatter in machine tools - demonstration with a "hardware in the loop" simulator. *Journal of Systems and Control Engineering, Proceedings of the Institution of Mechanical Engineers 219*(15), 359–369.

Glaser, D. J. Nachtigal, C. (1979). Development of a hydraulic chambered, actively controlled boring bar. *ASME Journal of Engineering for Industry 101*, 362–368.

Gradisek, J., M. Kalveram, T. Insperger, K. Weinert, G. Stepan, E. Govekar, and I. Grabec (2005). On stability prediction for milling. *International Journal of Machine Tools and Manufacture 45*, 769–781.

Hahn, R. S. (1951). Active dampers for machine tools. *Transactions of ASME 73*, 213–222.

Hoshi, T., N. Sakisaka, I. Moriyama, and M. Sato (1977). Study of practical application of fluctuating speed cutting for regenerative chatter control. *Annals of the CIRP 25*, 175–179.

Insperger, T., B. Mann, G. Stepan, and P. V. Bayly (2003a). Multiple chatter frequencies in the milling process. *Journal of Sound and Vibration 262*, 333–345.

Insperger, T., B. Mann, G. Stepan, and P. V. Bayly (2003b). Stability of up-milling and down-milling, part 1: Alternative analytical methods. *International Journal of Machine Tools and Manufacture 43*, 25–34.

Kondo, Y. Kawano, O. and H. Sato (1981). Behavior of self-excited chatter due to multiple regenerative effect. *ASME Journal of Engineering for Industry 103*, 324–329.

Lin, S. C. DeVor, R. E. and S. G. Kapoor (1990). The effects of variable speed cutting on vibration control in face milling. *ASME Journal of Engineering for Industry 112*, 1–11.

Mann, B., T. Insperger, P. Bayly, and G. Stepan (2003). Stability of up-milling and down-milling, part 2: Experimental verification. *International Journal of Machine Tools and Manufacture 43*, 35–40.

Mann, B. P., P. V. Bayly, M. A. Davies, and J. E. Halley (2004). Limit cycles, bifurcations and accuracy of the milling process. *Journal of Sound and Vibration 277*, 31–48.

Merdol, S. D. and Y. Altintas (2004). Multi frequency solution of chatter stability for low immersion milling. *ASME Journal of MAnufacturing Science and Engineering 126*(3), 459–466.

Merrit, H. E. (1965). Theory of self-excited machine-tool chatter-contribution to machine tool chatter research-1. *ASME Journal of Engineering for Industry 87*(4), 447–454.

Minis, I. Yanushevsky, R. (1993). A new theoretical approach for the prediction of machine tool chatter in milling. *ASME Journal of Engineering for Industry 115*, 1–8.

Miu, D. K. (1991). Physical interpretation of transfer function zeros for simple control systems with mechanical flexibilities. *Journal of Dynamic Systems, Measurement and Control, Transactions of the ASME 113*, 419–423.

Nachtigal, C. (1972). Design of a force feedback chatter control system. *ASME Journal of Dynamic Systems, Measurement and Control 94*(1), 5–10.

Preumont, A. (2002). *Vibration Control of Active Structures - An Introduction*. Kluwer Academic Publishers.

Schmitz, T. (2003). Chatter recognition by a statistical evaluation of the synchronously sampled audio signal. *Journal of Sound and Vibration 262*, 721–730.

SDTools. *Structural Dynamics Toolbox*. http://www.sdtools.com.

Segalman, D. and J. Redmond (1996). Chatter suppression through variable impedance and smart fluids. *Proceedings of the SPIE 2721*, 353–363.

Sexton, J. S. Stone, B. J. (1978). The stability of machining with continuosly varying spindle speed. *Annals of the CIRP 27*, 321–326.

Sims, N. and Y. Zhang (2003). Active damping for chatter reduction for high speed machining. *Proceedings of the AMAS workshop on smart materials and structures*, 195–212.

Slavicek, J. (1965). The effect of irregular tooth pitch on stability of milling. In *Proceedings of M.T.D.R.*

Smith, S. and J. Tlusty (1990). Update on high-speed milling dynamics. *ASME Journal of Engineering for Industry 112*, 142–149.

Smith, S. and J. Tlusty (1992). Stabilizing chatter by automatic spindle speed regulation. *Annals of the CIRP 41*(1), 433–436.

Smith, S. and J. Tlusty (1993). Efficient simulation programs for chatter in milling. *Annals of the CIRP 42*, 463–466.

Soliman, E. and F. Ismail (1998). A control system for chatter avoidance by ramping the spindle speed. *ASME Journal of Manufacturing Science and Engineering 120*, 674–683.

Sridhar, R., R. E. Hohn, and G. W. Long (1968a). A general formulation of the milling process equation. *ASME Journal of Engineering for Industry 90*, 317–324.

Sridhar, R., R. E. Hohn, and G. W. Long (1968b). A stability algorithm for the general milling process. *ASME Journal of Engineering for Industry 90*, 330–334.

Tarng, Y. S., J. Y. Kao, and E. C. Lee (2000). Chatter suppression in turning operations with a tuned vibration absorber. *International Journal of Materials Processing Technology 105*, 55–60.

Tlusty, J. (1978). Analysis of the state of research in cutting dynamics. *Annals of the CIRP 27(2)*, 583–589.

Tlusty, J. and F. Ismail (1981). Basic non-linearity in machining chatter. *Annals of the CIRP 30*(1), 299–304.

Tlusty, J. and F. Ismail (1983). Special aspects of chatter in milling. *ASME Journal of Vibration, Acoustics, Stress and Reliability in Design 105*, 24–32.

Tlusty, J. and P. Macneil (1975). Dynamics of cutting forces in end milling. *Annals of the CIRP 24*, 21–25.

Tlusty, J. and M. Polacek (1963). The stability of machine tools against self-excited vibrations in machining. *International Research in Production Engineering*, 465–474.

Tlusty, J., W. Zaton, and F. Ismail (1983). Stability lobes in milling. *Annals of the CIRP 32*(1), 309–313.

Tobias, S. and W. Fishwick (1958a). Theory of regenerative machine tool chatter. *Engineering 205*.

Tobias, S. A. and W. Fishwick (1958b). The chatter of lathe tools under orthogonal cutting conditions. *Transactions of the ASME 80*, 1079–1088.

Wiberg, D. (1971). *State Space and Linear Systems*. McGraw-Hill Book Company.

Zhang, Y. and N. Sims (2005). Milling workpiece chatter avoidance uisng piezoelectric active damping: a feasibility study. *Smart Materials and Structures 14*, N65–N70.